diabetes®
American Diabetes Association®

Exploring Structural and Molecular Features of Sciatic Nerve Lesions in Diabetic Neuropathy: Unveiling Pathogenic Pathways and Targets

Daniel Schwarz, Maxime Le Marois, Volker Sturm, Andreas S. Peters, Rémi Longuespée, Dominic Helm, Martin Schneider, Bastian Eichmüller, Asa S. Hidmark, Manuel Fischer, Zoltan Kender, Constantin Schwab, Ingrid Hausser, Joachim Weis, Susanne Dihlmann, Dittmar Böckler, Martin Bendszus, Sabine Heiland, Stephan Herzig, Peter P. Nawroth, Julia Szendroedi, and Thomas Fleming

Diabetes 2025;74(1):65–74 | https://doi.org/10.2337/db24-0493

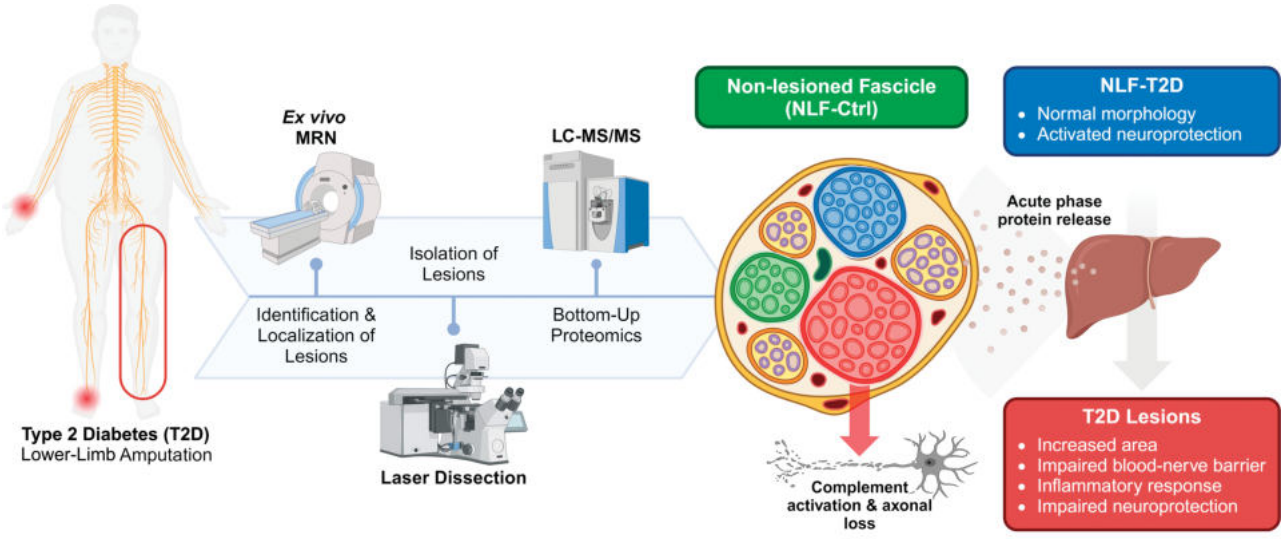

Ctrl, control; LC-MS/MS, liquid chromatography-tandem mass spectrometry; MRN, magnetic resonance neurography.

Exploring Structural and Molecular Features of Sciatic Nerve Lesions in Diabetic Neuropathy: Unveiling Pathogenic Pathways and Targets

Daniel Schwarz,[1] Maxime Le Marois,[2] Volker Sturm,[1] Andreas S. Peters,[3,4] Rémi Longuespée,[5] Dominic Helm,[6] Martin Schneider,[6] Bastian Eichmüller,[2] Asa S. Hidmark,[2] Manuel Fischer,[1] Zoltan Kender,[2,7] Constantin Schwab,[8] Ingrid Hausser,[8] Joachim Weis,[9] Susanne Dihlmann,[3] Dittmar Böckler,[3] Martin Bendszus,[1] Sabine Heiland,[1] Stephan Herzig,[7,10,11,12] Peter P. Nawroth,[2,13] Julia Szendroedi,[2,7,11] and Thomas Fleming[2,7,11]

Diabetes 2025;74:65–74 | https://doi.org/10.2337/db24-0493

Lesioned fascicles (LFs) in the sciatic nerves of individuals with diabetic neuropathy (DN) correlate with clinical symptom severity. This study aimed to characterize the structural and molecular composition of these lesions to better understand DN pathogenesis. Sciatic nerves from amputees with and without type 2 diabetes (T2D) were examined using ex vivo magnetic resonance neurography, in vitro imaging, and proteomic analysis. Lesions were only found in T2D donors and exhibited significant structural abnormalities, including axonal degeneration, demyelination, and impaired blood-nerve barrier (BNB). Although non-LFs from T2D donors showed activation of neuroprotective pathways, LFs lacked this response and instead displayed increased complement activation via the classical pathway. The detection of liver-derived acute-phase proteins suggests that BNB disruption facilitates harmful interorgan communication between the liver and nerves. These findings reveal key molecular mechanisms contributing to DN and highlight potential targets for therapeutic intervention.

ARTICLE HIGHLIGHTS

- Lesioned fascicles in the sciatic nerves of individuals with diabetic neuropathy correlate with clinical symptom severity.
- We aimed to investigate the structural and molecular composition of lesioned fascicles in patients with type 2 diabetes to better understand the mechanisms underlying diabetic neuropathy.
- Nonlesioned fascicles from nerves from individuals with type 2 diabetes activated neuroprotective pathways, whereas lesioned fascicles showed structural damage, impaired blood-nerve barrier, and complement activation.
- These findings suggest that targeting complement activation could offer therapeutic potential for diabetic neuropathy.

[1]Department of Neuroradiology, Heidelberg University Hospital, Heidelberg, Germany
[2]Department for Endocrinology, Diabetology, Metabolic Diseases and Clinical Chemistry, University Hospital Heidelberg, Heidelberg, Germany
[3]Department for Vascular Surgery and Endovascular Surgery, Heidelberg University Hospital, Heidelberg, Germany
[4]Vascular Biomaterial Bank Heidelberg, Heidelberg University Hospital, Heidelberg, Germany
[5]German Cancer Research Center (DKFZ) Heidelberg, Division of Metabolic Crosstalk in Cancer and the German Cancer Consortium (DKTK), DKFZ Core Center Heidelberg, Heidelberg, Germany
[6]Proteomics Core Facility, German Cancer Research Center (DKFZ), Heidelberg, Germany
[7]German Center for Diabetes Research (DZD), Helmholtz Center Munich, Neuherberg, Germany
[8]Department of General Pathology, Institute of Pathology, Heidelberg University Hospital, Heidelberg, Germany
[9]Institute of Neuropathology, Rheinisch-Westfälische Technische Hochschule (RWTH) Aachen, University Hospital, Aachen, Germany
[10]Institute for Diabetes and Cancer, Helmholtz Center Munich, Neuherberg, Germany
[11]Joint Heidelberg-Institute for Diabetes and Cancer (IDC) Translational Diabetes Program, Internal Medicine I, Heidelberg University Hospital, Heidelberg, Germany
[12]Chair Molecular Metabolic Control, Technical University Munich, Munich, Germany
[13]Institute for Immunology, University Hospital Heidelberg, Heidelberg, Germany

Corresponding author: Thomas Fleming, thomas.fleming@med.uni-heidelberg.de

Received 14 June 2024 and accepted 30 September 2024

This article contains supplementary material online at https://doi.org/10.2337/figshare.27233751.

Diabetic neuropathy (DN) is a prevalent and severe complication of diabetes, affecting individuals at risk as well. The progression of DN involves structural changes in the distal and proximal peripheral nerves and microcirculatory dysfunction, including endoneurial microangiopathy and endothelial dysfunction (1,2). Risk factors for DN include hypertension, smoking, hyperglycemia, diabetes duration, age, dyslipidemia, and obesity, which are consistent with those factors identified for the presence and, more significantly, the progression of metabolic dysfunction-associated steatotic liver disease (MASLD) (3). In its more severe form, MASLD may therefore contribute to the progression of DN (4).

High-resolution magnetic resonance neurography (MRN) has revealed fascicle lesions (FLs) in the proximal sciatic nerve trunk. These lesions are characterized by hyperintense monofocal or multifocal patterns, predominantly occurring at the thigh level (5,6). Elevated lesion loads correlate with the severity of clinical symptoms and impaired nerve conduction parameters, with the loss of sensory function, as assessed by quantitative sensory testing (7) and with glycated hemoglobin (HbA_{1c}) (8). Diffusional parameters derived from MRN, such as decreased fractional anisotropy (FA), indicate nerve fiber integrity and are established for the noninvasive assessment of neuronal microstructure. Previous studies have shown that FA negatively correlated with neuropathy deficit scores and positively with nerve conduction velocity, remaining significant even after adjusting for age, sex, BMI, and HbA_{1c} (9,10). Additionally, FA exhibits negative correlations with neurofilament light chain (NFL), a biomarker of neuroaxonal damage seen across various neurodegenerative diseases, including DN (11).

MRN can therefore serve as a valuable diagnostic tool for noninvasively assessing nerve function, surpassing the limitations of standardized tests such as questionnaire-based assessments or clinical examination, which are subjective and dependent on individual cooperation (1). In contrast, MRN provides a more objective assessment, particularly beneficial for tracking the natural progression of the disease, pinpointing biomarkers, and gauging the efficacy of interventions aimed at personalized medicine. However, the histomorpholgical and molecular nature of the lesions remains unexplored, hindering our understanding of their role in DN pathogenesis. Although studies have suggested that these lesions could represent enhanced posttranslational modifications of extracellular matrix proteins within the neuronal compartment (5,6), direct evidence is lacking. This gap in understanding partly stems from reliance on postmortem analyses, because animal models do not perfectly replicate the human condition (1,12).

In this study, we assessed the morphological and molecular nature of sciatic lesions in patients with DN. Sciatic lesions identified via in vivo imaging were analyzed involving ex vivo imaging and histological and molecular analysis of sciatic nerves obtained after lower-limb amputation from individuals with and without type 2 diabetes (T2D). By using comparative spatial proteomic analysis (13,14), we provide, for the first time, a comprehensive description of the structural and molecular composition of lesions to better understand their role in the pathogenesis of DN.

RESEARCH DESIGN AND METHODS

Collection of Human Nerve Tissue

A total of 11 sciatic nerves were obtained from individuals with T2D undergoing major lower-limb amputation due to ischemia and/or infection. In addition, four sciatic nerves from individuals without T2D and without identifiable lesions were also analyzed. All participants provided written informed consent, and the study was approved by the University of Heidelberg Ethics Committee (No. S-279/2018, S-281/2018, and S-301/2013) and conducted in accordance with the Declaration of Helsinki 2013. The characteristics of the study cohort are summarized in Table 1.

Freshly dissected sciatic nerves were immediately stored in DMEM/Nutrient Mixture F-12 (Thermo Fisher, Waltham, MA) and placed on ice. To establish origination of the structures described by the MRN imaging, a suture was placed at the proximal end of the nerve. To establish the presence of neuropathic features of DN on the ultrastructural level, fascicles from the distal end were isolated for electron microscopy analysis, and the remaining tissue was directly transferred for MRN imaging and downstream processing (Supplementary Fig. 1).

MRI Data Acquisition

MRN imaging was performed at room temperature using a clinical 3 Tesla magnetic resonance scanner (Magnetom Trio, Siemens, Erlangen, Germany) equipped with a 15-channel transmit-receive knee coil and, subsequently, a 9.4 Tesla horizontal bore small-animal NMR scanner (BioSpec 94/20 USR, Bruker BioSpin GmbH, Ettlingen, Germany) with a four-channel phased-array surface receive coil, as previously described (12).

Laser Microdissection and Sample Processing

Individual fascicles, excluding the perineurium, were dissected from formalin-fixed paraffin-embedded sections (5 μm) and collected using an LMD7000 platform (Leica Microsystems). Per sample, a pooled amount number of fascicles were collected based on a common area of 450,000 μm^2. The samples were then processed for analysis by liquid chromatography–tandem mass spectrometry, as previously described (15), which was performed for 90 min using an Ultimate 3000 UPLC system and an Orbitrap Exploris 480 mass spectrometer (both Thermo Fisher Scientific) in data-dependent mode.

Data and Resource Availability

Detailed protocols for the methods used in study are provided in the supplementary information. The data sets generated during and/or analyzed during the current study are available from the corresponding author upon reasonable request.

Table 1—Baseline characteristics of study participants

Parameter	No diabetes, NLF-Ctrl (n = 4)	T2D without lesions, NLF-T2D (n = 4)	T2D with lesions, LF-T2D (n = 7)
Age (years)	65 ± 5	63 ± 10	75 ± 10
Sex (male/female), *n*	2/2	3/1	1/6
BMI (kg/m^2)	21.2 ± 4.6	26.6 ± 1.8	26.5 ± 5.4
Diabetes duration (years)	N/A	12.5 ± 5.3	10.5 ± 6.7
Blood glucose (mg/dL)	106 ± 35	164 ± 89	130 ± 40
Complications (yes/no), *n*			
Cardiovascular disease	2/4	4/4	5/7
Retinopathy	0/4	2/4	3/7
Nephropathy	1/4	3/4	5/7
Neuropathy	0/4	2/4	7/7
Lesions (yes/no)	N/A	0/4	7/7
Reason for amputation	Ischemia/infection	Ischemia/infection	Ischemia/infection
Ischemia/infection status	Localized/systemic	Localized/systemic	Localized/systemic

Data are presented as mean ± SD unless indicated otherwise as *n*. N/A, not applicable.

RESULTS

Study Participants

Included were 11 individuals with T2D (9 men/2 women, aged 76.0 [interquartile range 68.0, 81.0] years) and 4 individuals without T2D (2 men/2 women, aged 61.0 [interquartile range 54.5, 72.8] years). All participants underwent major lower-limb amputation due to ischemia and/or infection and were enrolled at the time of the surgical intervention. The diagnosis of diabetes was confirmed based on medical records. No significant differences in age, sex, or baseline characteristics were observed between the T2D and non-T2D groups (Table 1). Although complications such as cardiovascular disease, retinopathy, nephropathy, and neuropathy were present among participants, the prevalence of these complications did not significantly differ between the groups with and without T2D. Ultrastructural analysis shows that the nondiabetic nerves exhibited both normal myelinated and unmyelinated nerve fibers at a regular density. In contrast, nerves from individuals with T2D showed a spectrum of distinct ultrastructural changes commonly associated with moderate-to-severe chronic neuropathy (1,2) (Supplementary Figs. 2 and 3). To identify LFs and their location within the nerve, macrostructural analysis via ex vivo MRN imaging was performed.

Identification of Fascicular Lesions by MRN

Assessment of the MRN images showed the presence of phenotypical T2-w hyperintense fascicular nerve lesions only in T2D but not in amputees without diabetes (Fig. 1*A–D*). To quantitatively define the lesions, the T2 times from all fascicles were fitted to a two-component gaussian-mixture-model. With a cutoff of 37.6 ms, two clusters could be defined as either non-lesioned fascicles (NLFs) ($\mu1$ = 25.4; $\sigma1$ = 4.7) or LFs ($\mu2$ = 46.6; $\sigma2$ = 5.5) (Fig. 1*E*). Accordingly, 19.5% of all fascicles of amputees with T2D were classified as LFs, which were subsequently found to have additional distinct differences in the other quantitative imaging parameters, as compared to NLF (Fig. 1*F–H* and Supplementary Table 1).

Morphological Characterization of Fascicular Lesions

LFs exhibited a significant increase in fascicular area and a thinner perineurium (Fig. 2*A*), indicative of increased interstitial space often containing a higher deposition of acid mucins. These characteristics are consistent with endoneurial edema and compromise of the blood-nerve barrier (BNB). Immunofluorescence analysis revealed a significant loss of both myelinated and neurofilament light axons in LFs compared with NLFs (Fig. 2*B–D* and Supplementary Table 1), consistent with neurodegeneration. Correspondingly, the MRN parameter FA, also a marker of fiber integrity, exhibited a significant decrease (Supplementary Table 1), further supporting this observation.

Correlation analysis with hyperintensities, measured by T2 time, demonstrated that LFs were positively associated with increased fascicular area and Alcian blue–periodic acid Schiff (AB-PAS) grading and were negatively associated with perineural thickness (Supplementary Table 1). This suggests a direct relationship between histological changes in LFs and neurodegeneration in DN, underscoring the clinical relevance of LFs. Moreover, these findings highlight the potential of histological examination in identifying and characterizing LFs, even in the absence of MRN.

Microproteomic Analysis of Nerve Fascicles

After identifying and characterizing LFs compared with NLFs, a comparative analysis of the proteome was performed. Of the 11 T2D individuals, 4 had no detectable sciatic nerve lesions. These four individuals were analyzed as a separate group, independent from the seven individuals with lesions. Their results were not combined with

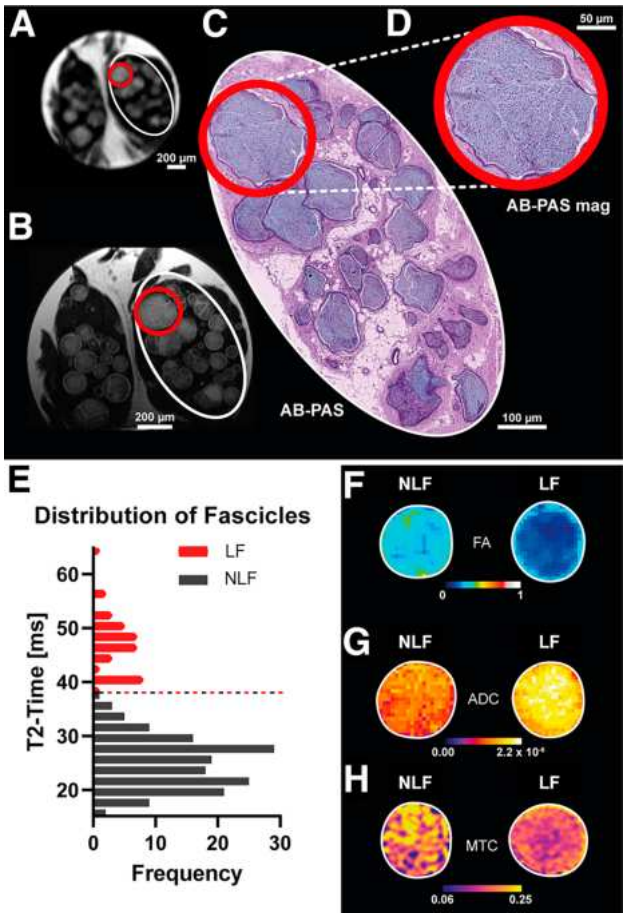

Figure 1—MRN of FLs. Clinical resolution T2-weighted MRN at 3 Tesla, individual nerve fascicles can be visualized within the sciatic nerve with typical hyperintensity of nerve lesions (red circle). *A*: At 9.4 Tesla ultra-high-field MRN, subfascicular internal structures of the same specimen are visible with a corresponding diffuse hyperintensity of fascicular nerve lesions. Corresponding histomorphology of the tibial portion of the sciatic nerve (white ellipsoid in *A*–*C*) (*B*) in the AB- PAS staining (*C*). *D*: Magnified MRN identified fascicular nerve lesion (red circle) corresponding to increased fascicular AB positivity. *E*: An unbiased approach based on a two-component gaussian-mixture-model applied to T2 time was used to identify nerve lesions (red bars) on MRN above a threshold value of 37.6 ms (dashed line). Fascicles below this threshold were considered as NLFs (black bars), whereas fascicles above this threshold were considered as LFs (red bars). *F*: On multiparametric quantitative MRN, DN nerve lesions exhibit the same MR morphotype compared with in vivo findings. An example pair of NLFs and LFs shows a typical decrease of fractional anisotropy (FA) (*F*), increase of apparent diffusion coefficient (ADC) (*G*), and a decrease of magnetization transfer contrast (MTC) (*H*).

those from the lesioned group in the subsequent molecular analyses. No significant differences in age, sex, BMI, or baseline characteristics were observed between the T2D and T2D lesion groups. However, the frequency of neuropathy was higher in the T2D lesion group (Table 1).

From the seven T2D sciatic nerves with lesions, 60 LFs (LF-T2D) were isolated by laser microdissection, along with 10 NLFs (NLF-T2D) for the four T2D sciatic nerves without lesions. Additionally, 10 NLFs from the four sciatic nerves of patients without diabetes (NLF-Ctrl) were also isolated for analysis. Across the groups, a consistent number of proteins were detected (Supplementary Fig. 4*A*), similar to levels detected in similar microproteomic approaches (15). Substantial similarities ($P > 0.05$) were observed in the subcellular localization and cellular molecular function among the groups (Supplementary Fig. 4*B*). The lack of substantial differences suggests that the observed lesions do not represent significant proteolytic stress.

Comparative Analysis of the Fascicular Lesion Proteome

A total of 346 proteins were shared among all three groups (Fig. 3*A*). Principal component analysis (PCA) revealed that 34% of the differences lay between the groups, with most data points clustering within the 0.95 Hotelling ellipse (Fig. 3*B*). Hierarchical clustering confirmed overlap among the groups (Fig. 3*C*). Notable proteomic differences were observed, particularly between NLF-Ctrl and LFs-T2D, whereas NLF-Ctrl and NLF-T2D clustered more closely. Comparative analysis of the shared proteins (Fig. 3*D*) showed 6 differentially changed proteins in NLF-T2D compared with the NLF-Ctrl (Supplementary Table 2) and a total of 40 proteins in LFs-T2D, 28 proteins compared with NLF-Ctrl (Supplementary Table 3*A*), and 12 proteins comparted with NLF-T2D (Supplementary Table 3*B*). Four proteins were upregulated and two downregulated in NLF-T2D, with no significant interactions or functional clusters identified. In LF-T2D, 17 proteins were uniquely upregulated, associated with complement activation and acute-phase response clusters (Supplementary Fig. 5*A*). Additionally, 23 proteins were uniquely downregulated, associated with cytoplasmic translational and protein processing clusters (Supplementary Fig. 5*B*). Between NLF-T2D and LF-T2D, 14 uniquely shared proteins were identified, with 12 upregulated and 2 downregulated in both groups (Supplementary Table 4). These proteins are therefore indicative of T2D-specific changes. A functional cluster associated with complement activation and coagulation cascades was observed for the upregulated proteins (Supplementary Fig. 5*C*). Additionally, two proteins—α-1-microglobulin (upregulated) and biliverdin reductase B (downregulated)—were found to be specific to LF-T2D (Supplementary Table 3*A* and *B*). In relation to the complement activation, analysis of label-free quantification intensities confirmed this, revealing a significant increase in abundance of complement components 3 (C3) and 9 (C9), along with several immunoglobulin subtypes, in LF-T2D compared with NLF-Ctrl (Supplementary Table 5). Furthermore, CD59 or protectin, a negative regulator of the complement pathway, was found to be significantly decreased in LF-T2D compared with both NLF-Ctrl and NLF-T2D (Supplementary Table 5).

Each group exhibited a distinct set of uniquely detected proteins (Fig. 3*A*): 32 proteins in the NLF-Ctrl (Supplementary Table 6*A*), 37 proteins in the NLF-T2D

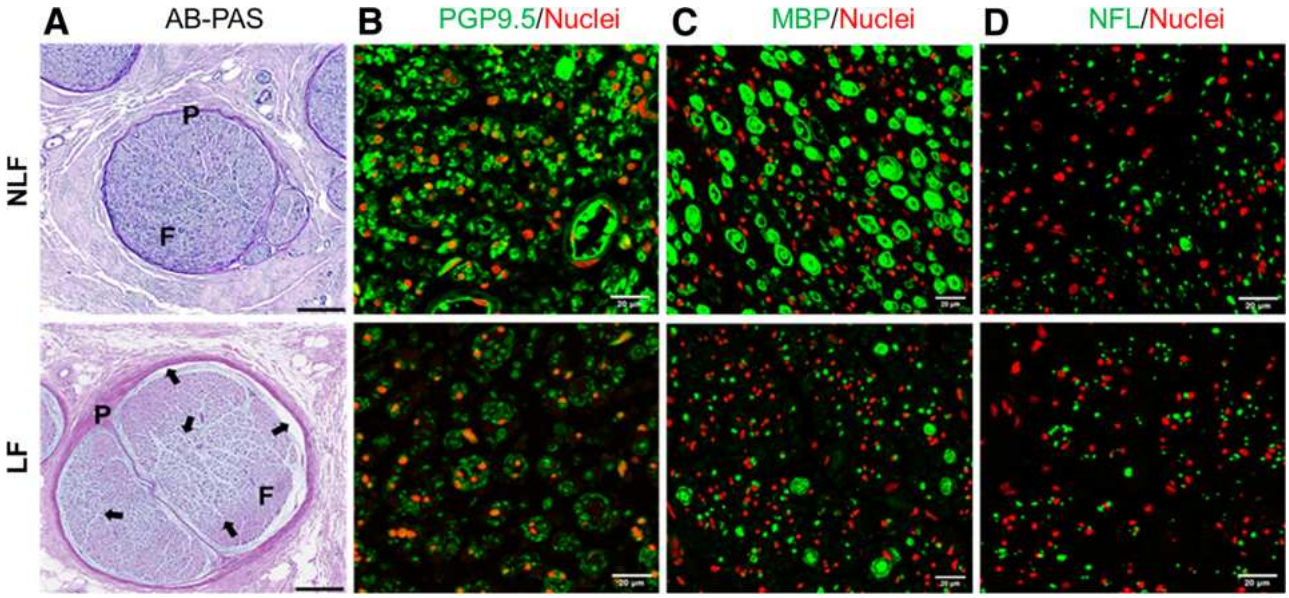

Figure 2—Morphological characterization of NLFs and LFs. *A*: Representative images of NLFs and LFs stained with AB-PAS. Lesions were visually larger and less compact and showed indications of having increased interstitial spaces. These spaces either remained emptied or contained mucin depositions (black arrows). F, fascicle body; P, perineurium. Scale bar = 200 μm. Immunofluorescent analysis of NLFs and lesions for the neuronal markers, neuron cytoplasmic protein gene product 9.5 (PGP9.5) (*B*), myelin basic protein (MBP) (*C*), and neurofilament-light (NFL) (*D*). Fascicles were stained for the specified neuronal marker (green) and nuclei (red), as described in *Research Design and Methods*. Images were acquired on a Nikon A1R confocal microscope with a 10× objective (scale bar = 20 μm).

(Supplementary Table 6*B*), and 43 proteins in the LF-T2D (Supplementary Table 6*C*). Because these proteins are exclusive to each group, direct comparison between them is not feasible. However, interaction analysis can uncover relevant functional implications. In the NLF-Ctrl group, three functional clusters were identified: the endomembrane system, translational regulator activity, and extracellular exosomes (Supplementary Fig 6*A* and Supplementary Table 7*A*). These functional clusters likely represent important basal molecular processes specific to the nerve compartment. The unique proteins detected in NLF-T2D were associated with transport processes from intracellular to extracellular compartments as well as focal adhesion processes (Supplementary Fig. 6*B* and Supplementary Table 7*B*). In contrast, the uniquely detected proteins in LF-T2D were functionally associated with the negative regulation of cholesterol import and VLDL remodelling. Furthermore, the complement pathway once again emerged as a functionally relevant pathway in LF-T2D (Supplementary Fig. 6*C* and Supplementary Table 7*C*).

Pathway Analysis

The comparative analysis revealed that although differences and similarities exist between NLF-Ctrl and NLF-T2D, LF-T2D stands out, and no single biomarker for diagnosing LFs could be reliably identified. This is partly due to the heterogeneity of the cellular environment within fascicles and lesions. Functional network enrichment was therefore conducted to explore proteomic differences within LF-T2D and investigate potential functional implications (Fig. 4). Regardless of the group comparison, the differences observed were strongly associated with neurological disease, organismal injury and abnormalities, and skeletal muscle disorder based on relative scoring; the network score was 43 for NLF-Ctrl versus NLF-T2D, was 38 for NLF-Ctrl versus LF-T2D, and was 39 for the comparison of NLF-T2D versus LF-T2D, consistent with the homogeneity observed with the PCA and hierarchical clustering (Fig. 3).

Activation of the liver X receptor–retinoid X receptor (LXR-RXR) signaling axis and downregulation of the unfolded protein response (UPR) are common pathways across all comparisons, indicating their specificity to T2D (Fig. 4*A* and *B*). In the NLF-Ctrl versus NLF-T2D comparison, activation of the pentose phosphate pathway (PPP), protein kinase A (PKA) signaling, and aldo-keto reductase (AKR)/aldehyde dehydrogenase (ALDH) metabolism were also specific to T2D (Fig. 4*A*). LF-T2D exhibits specific activation of acute phase response (APR) and glycoprotein-VI (GPVI) signaling pathways, with the highest enrichment observed in the NLF-T2D versus LF-T2D comparison (Fig. 4*B* and *C*). Additionally, LF-T2D shows specific activation of endothelial nitric oxide (NO) synthase (eNOS) signaling, present in comparisons involving LF-T2D (Fig. 4*B* and *C*). Other canonical pathways identified as specific to the lesions included the activation of the intrinsic prothrombin and idiopathic pulmonary fibrosis signaling pathways as well as the downregulation of energy metabolism (Fig. 4*C*).

DISCUSSION

In this study, we provide, for the first time, a comprehensive description of the structural and molecular composition

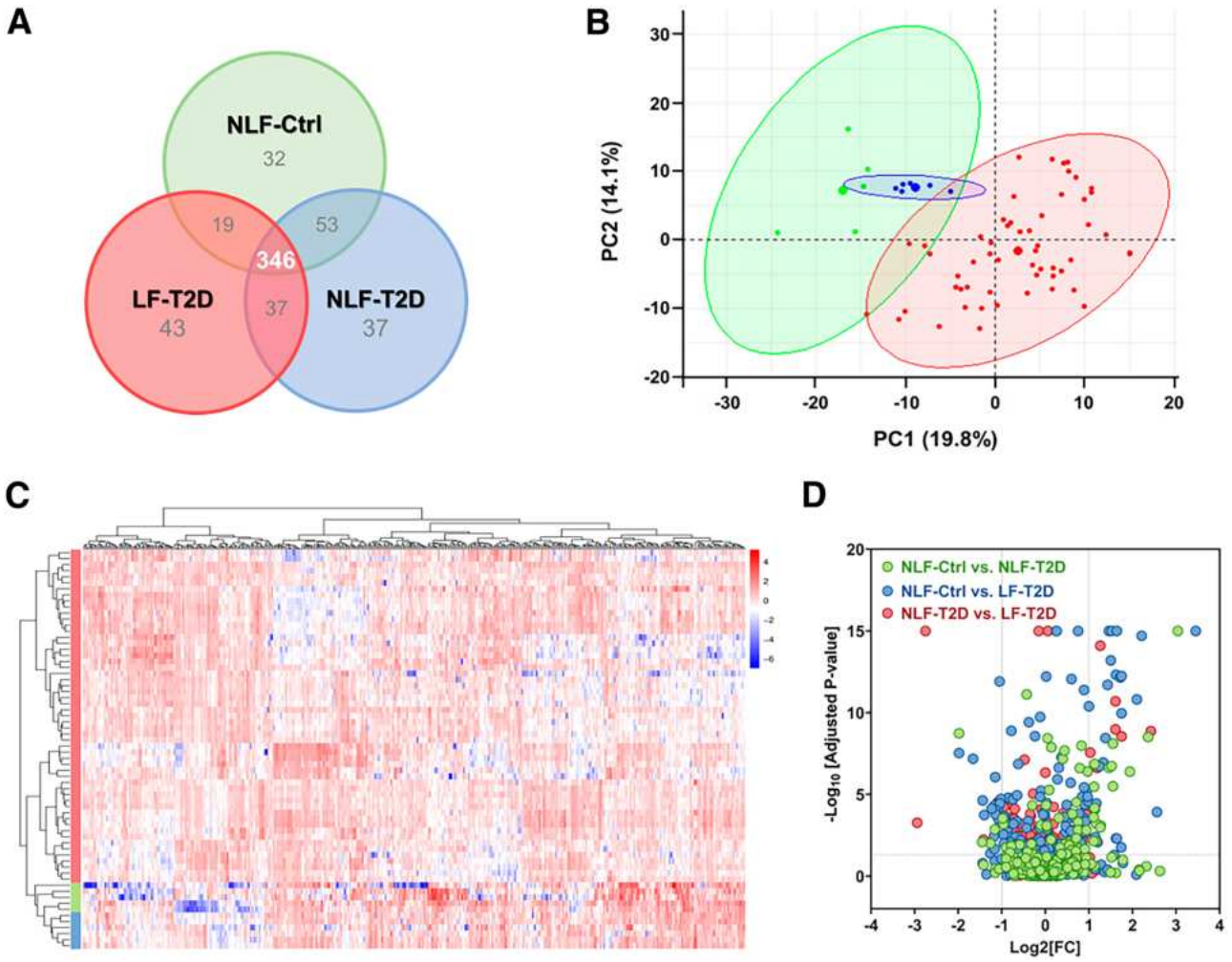

Figure 3—Microproteomic analysis of lesioned fascicles. *A*: Venn diagram shows the overlap in the number of identified proteins in NLF-Ctrl, NLF-T2D, and LF-T2D. *B*: PCA of the 346 proteins shared in all three groups. *C*: Hierarchical heat map cluster of the 346 proteins shared in all three groups. *D*: Volcano plot of the differential changes in 346 proteins across all three groups. Vertical dotted lines represent the $\log_2$[fold-change (FC)] cutoff values, and the horizontal dotted lines represent the $-\log_{10}$[adjusted *P* value] cutoff values.

of sciatic nerve lesions associated with DN. Sciatic nerves of individuals with T2D without lesions show no morphological differences related to T2D but do exhibit activation of neuroprotective pathways compared with individuals without diabetes. However, LFs lack these pathways and display structural abnormalities, including reduced fiber integrity, axonal degeneration, demyelination, and signs of impaired BNB. Spatial proteomics revealed enrichment in proinflammatory and complement activation pathways in LFs. Many proteins associated with these pathways, specifically in the APR, originate from the liver. This suggests that impaired BNB function facilitates harmful interorgan communication between the nerve and the liver. Furthermore, in T2D, this communication may be exacerbated by the onset of MASLD (3).

The integration of structural and molecular analyses enhances our understanding of sciatic nerve lesions in the pathogenesis of DN, thereby facilitating the development of targeted therapeutic strategies. Moreover, these findings underscore the importance and utility of noninvasive MRN in clinical studies, because it now allows for correlations with ex vivo morphological studies, providing valuable insights into the underlying mechanisms of DN. Such lesions, previously identified by MRN in individuals with DN, have been found to occur in a proximal-to-distal gradient, correlating with the severity of clinical symptoms (5–10). This study identified three types of fascicles based on T2-weighted signals: NLF-Ctrl, NLF-T2D, and LF-T2D. The latter accounts for 20% of the measured fascicles, consistent with previous findings (7,8). LF-T2D exhibited a reduction in FA, a critical marker for fiber integrity (5–9,12), and displayed a significant increase in fascicle area and perineurium thinning. Such characteristics positively correlated with MRN parameters, indicating an association with morphological differences. There was also a significant decrease in the number of myelinated fibers within the LFs, suggesting axonal degeneration and/or demyelination. This aligns with the reduction in FA and is consistent with previous studies showing that increased

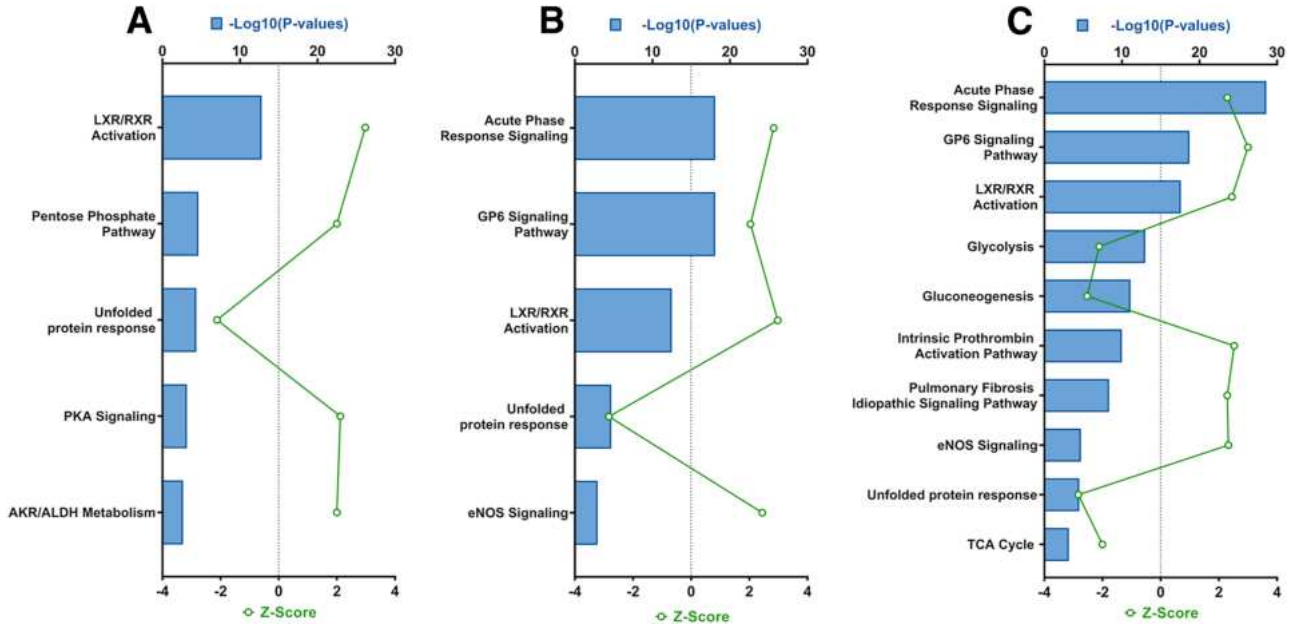

Figure 4—Functional enrichment analysis. NLF-Ctrl vs. NLF-T2D (*A*); NLF-Ctrl vs. LF-T2D (*B*); and NLF-T2D versus LF-T2D (*C*). TCA, tricarboxylic acid cycle.

lesion load is associated with sensory loss (7). Additionally, LFs showed increases in interstitial spaces, suggesting endoneurial edema and a compromise of the BNB, consistent with findings that have demonstrated altered capillary permeability in DN (16).

To gain insight into the pathophysiology of LF-T2D relative to the NLF-Ctrl or NLF-T2D, spatial proteomics was performed. This method involves analyzing protein abundances across various cellular and subcellular compartments, achieved through the use of laser capture microdissection (13,14). It offers a significant advantage because it does not rely on prior knowledge of specific molecular targets. Instead, spatial proteomics depends on functional network enrichment, categorizing identified proteins based on their functions using statistical overlap analysis. This methodology was crucial for the study's objective, aiming to elucidate molecular pathways and their functional activation concerning morphological changes, rather than solely focusing on identifying biomarkers for diagnosing LFs. Furthermore, the suitability of formalin-fixed and paraffin-embedded clinical samples for such an approach is notable (13,14).

This analysis revealed that NLF-Ctrl and NLF-T2D clustered closely together, consistent with the lack of any morphological changes. However, functional network enrichment analysis indicated the activation of molecular pathways supporting regeneration in the NLF-T2D. Particularly, the LXR/RXR signaling pathway, known for its pivotal role in regulating lipid metabolism (17), exhibited enhanced activity. Axonal degeneration and regeneration, crucial for nerve injury recovery, are mediated by tissue-resident macrophages and Schwann cells (SCs). Macrophages are responsible for myelin phagocytosis, whereas SCs contribute to remyelination. Because myelin is lipid-rich (18), modulating lipid metabolism—whether for degradation by macrophages or synthesis by SCs—is essential for successful axonal recovery. The role of activation of the LXR/RXR pathway in NLF-T2D could be to counter excessive cellular cholesterol accumulation during demyelination by upregulating sterol transporters and transcription factors (17). Additionally, the LXR/RXR pathway demonstrates anti-inflammatory effects in atherosclerosis and neuroinflammation (19–21).

Several neuroprotective pathways were notably activated in the NLF-T2D. For instance, PKA activation has been shown to support axonal growth and regeneration after nerve injury (22). The PPP, a branch of glucose metabolism, is crucial for producing the reducing cofactor NADPH. Activation of PPP through thiamine supplementation or the lipid-derived analog benfotiamine has been shown to have protective effects in DN (23). NADPH is also pivotal in regenerating oxidized glutathione, a marker of oxidative stress, which has been long implicated in the development of DN. The activation of AKR/ALDH metabolism is also consistent with increased oxidative stress (1,2). These findings suggest that NLF-T2D shows no morphological differences compared with NLF-Ctrl at the molecular level, which supports axonal degradation/regeneration.

In contrast, notable differences were observed between NLF-Ctrl and LF-T2D, consistent with the structural disparities. None of the neuroprotective pathways, except for the LXR/RXR signaling pathway, were found to be enriched in LF-T2D. The degree of enrichment and activation of this pathway was equivalent to that observed in NLF-T2D; however, the beneficial effects on lipid metabolism were not evident due to the reduction in both

unmyelinated and myelinated axons compared with NLF-T2D. The absence of regenerative processes might be due to the lack of neuroprotective pathways, but it may also be a consequence of the loss of UPR. T2D is associated with reduced heat shock factor-1 (Hsf-1) and diminished expression of Hsp (24). The loss of Hsp disrupts the balance between axonal degeneration and regeneration by allowing aggregate formation and promoting proinflammatory responses (25). Because the loss of UPR was similar in both NLF-T2D and LF-T2D, it appears to be specific to the diabetic condition.

Functional analysis in the LF-T2D revealed specific enrichment of the GPVI signaling pathway and the APR. Both pathways have been reported to be active as part of a proinflammatory response to tissue injury (26,27). In particular, the APR, which primarily originates from the liver, has been demonstrated to be rapidly activated in models of peripheral nerve crush injury, thereby promoting nerve regeneration (28–30). The overrepresentation of these pathways within LF-T2D could therefore suggest a disruption to the BNB (31), consistent with histological findings suggestive of endoneurial edema. The underlying mechanism for this could be the activation of eNOS signaling. Although protein levels of eNOS or other NOS isoforms were not changed, a notable decrease in Hsp90 was observed. Hsp90 is crucial for eNOS activation and NO release (32). This decrease could lead to impaired vasorelaxation in capillary networks within the endoneurium, contributing to the development of microangiopathy within the fascicle body (33).

Complement proteins were significantly enriched in all samples. Although crucial to the innate immune system, SCs also highly express complement proteins (34). C3 was the most abundant and significantly elevated in NLF-T2D and LF-T2D compared with NLF-Ctrl, with no significant differences in the upstream regulators, indicating activation via the alternative pathway. In LF-T2D, several immunoglobulin subtypes were also enriched, likely due to BNB disruption or local production following immune cell recruitment. These IgG subtypes would generate immune complexes that activate complement. Thus, complement activation in NLF-T2D occurs mainly through the alternative pathway, whereas BNB disruption in LF-T2D leads to classical pathway activation. The interaction between SCs and immune cells may critically impact axon regeneration, because activated immune cells would trigger uncontrolled complement system activation in SCs, intensifying axonal damage.

C9, the second most abundant complement, was significantly elevated in LF-T2D, although to a lesser extent than C3. The presence of C9 indicates the formation of the membrane attack complex (MAC), which plays a critical role in nerve demyelination (35). CD59, a MAC inhibitor, was significantly reduced in LF-T2D. The downregulation of CD59 is linked to impaired recovery from spinal cord injury (36,37), and its loss in LF-T2D may explain the observed differences in functional and morphological pathways compared with NLF-T2D fascicles. While complement activation in NLF-T2D facilitates axonal degeneration and regeneration, the terminal effects of the MAC are inhibited by CD59. In LF-T2D, the complement cascade is enhanced by classical pathway activation via autoantibodies, and the loss of CD59 leads to excessive MAC activation, ongoing neuronal cell death, and axonal loss. The mechanism for the loss of CD59 is unclear but may involve glucose-dependent glycation (38).

Traditionally, DN treatments target hyperglycemia-mediated cellular injury, offering limited symptom relief. The NLF-T2D showed evidence of such pathway activation; however, inhibition could be detrimental in terms of neuroprotection. Treatment strategies should aim to activate these neuroprotective pathways before lesion formation. For example, the synthetic LXR ligand GW3965 has shown beneficial effects on LXR/RXR pathway activation in DN and other nerve injuries (19–21), while thiamine derivatives have demonstrated protection against DN (23). The molecular events leading to the neuroprotective pathway activation and the transformation from NLF-Ctrl to NLF-T2D remain unclear. Findings from LF-T2D suggest that targeting complement activation could be more effective. Anticomplement therapeutic strategies, such as eculizumab, ravulizumab, and PMX53, which prevent MAC formation, have been effective in various neurological diseases (39). In DN, complement suppression would reduce the inflammatory aspects of the lesions rather than alleviating neuropathic symptoms and should be used once the lesion load reaches a critical threshold. However, prolonged complement suppression may increase susceptibility to bacterial infections and should therefore be used with careful consideration.

Previous DN studies have been limited to skin biopsy specimens, postmortem sciatic nerve analysis, or animal models that do not perfectly replicate the human condition (1). Therefore, sciatic nerve material from living donors offers a unique opportunity to investigate the molecular mechanisms of DN. However, the nerves used in this study were from individuals who underwent lower-limb amputation due to ischemia and/or infection, representing an extreme proinflammatory condition that could influence the proteomic results. Given that all participants underwent lower limb amputation due to ischemia and/or infection, systemic inflammation and associated conditions likely influence the proteomic results, which could confound the interpretation of DN-specific pathways.

Despite the overlap in ischemic and infectious conditions among participants, our cohort data showed that those with neuropathic symptoms also presented with distinct lesions in their sciatic nerves. This suggests that while ischemia and infection are present in all participants, the presence of neuropathy is associated with additional structural and molecular abnormalities. However, the relatively small sample size and reliance on participants with advanced ischemia or infection

still limit the broader applicability of these findings. Future studies should aim to include control groups without such extreme proinflammatory conditions, such as traumatic amputees, to better isolate the effects of diabetes. Furthermore, larger and more diverse cohorts would be essential to validate the findings and ensure the generalizability of the results across different patient populations.

In addition to addressing cohort limitations, a more thorough exploration of the molecular mechanisms underlying these findings is necessary. While this study identifies key pathways involved in DN, such as complement activation and the acute phase response, a deeper investigation is required to fully understand how these pathways drive disease progression. The complexity of DN pathogenesis, alongside the limitations of current proteomic techniques, makes it challenging to identify specific upstream regulators and downstream effectors. Future research should use broader molecular analyses to further explore the roles of these pathways in neurodegeneration.

Complementing these molecular studies, longitudinal assessments that track DN progression—using MRN imaging to monitor lesion formation and correlate with neuropathic symptoms over time—could offer valuable insights into how DN evolves before severe ischemic or infectious conditions arise. Integrating such imaging techniques with molecular validation methods, such as transcriptomics and immunofluorescence, would provide a more comprehensive understanding of DN progression. Although these analyses were not feasible in this study due to resource constraints, they remain essential for validating the central findings and expanding our knowledge of DN pathogenesis.

Ex vivo MRN imaging provides an accurate representation of the in vivo situation (12) but cannot assess parameters such as perfusion and permeability, which are required for evaluating vascular integrity (16). In this context, in vivo microcirculatory studies in surgically exposed nerves, as demonstrated previously (40), could be applied in participants before amputation. This would allow for real-time assessment of microvascular deficits, providing valuable data that could complement the ex vivo analysis. The incorporation of such in vivo techniques in future studies would enhance our understanding of the role of microvascular dysfunction in DN.

In conclusion, this study offers a detailed examination of the structural and molecular composition of sciatic nerve lesions in DN. Unlike T2D nerves without lesions, LFs showed no neuroprotective pathway activation and exhibited reduced fiber integrity, axonal degeneration, demyelination, and impaired BNB function. Proteomic analyses highlighted marked differences between LFs and NLFs, particularly in inflammatory and complement activation pathways. Complement activation in NLF-T2D nerves primarily followed the alternative pathway, whereas LFs experienced classical pathway activation leading to significant neuronal damage due to CD59 absence. Additionally, inflammation-related proteins, notably APR from the liver, suggested BNB dysfunction, promoting detrimental interorgan communication that could exacerbate DN, especially when compounded by liver impairment as seen in MASLD (3). This is consistent with studies linking MASLD with DN progression in T2D (4). Future research should explore whether improving liver function could slow DN progression. Effective therapeutic strategies might include targeting BNB disruption and complement activation while enhancing neuroprotection. Further investigations are needed to clarify BNB impairment mechanisms, complement dysregulation, and the role of MASLD in DN. Understanding the transformation of NLF in diabetes is also crucial for future research. This study signifies a significant advancement in understanding the role of sciatic nerve lesions in DN pathogenesis.

Funding. This study was supported by the Deutsche Forschungsgemeinschaft (DFG; SFB1118, SFB1158 and GRK 1874/2 DIAMICOM) and the German Centre for Diabetes Research (DZD).

Duality of Interest. No potential conflict of interest relevant to this article were reported.

Author Contributions. D.S., M.L.M., P.P.N., and T.F. designed experiments. D.S., V.S., M.F., Sa.H., and M.B. provided MRN acquisition and image analysis. D.S. and T.F. wrote the manuscript. M.L.M., A.S.P., A.S.H., Z.K., S.D., D.B., and T.F. contributed to identification, collection, and processing of human sciatic materia. M.L.M. and R.L. performed laser microdissection and preanalytical processing. D.H., M.S., and B.E. conducted the mass spectrometry and data analysis. A.S.H., C.S., I.H., and J.W. performed histological (light and electron microscopy) analysis. M.B., St.H., P.P.N., and J.S. provided critical feedback. All authors approved the final version of the manuscript. T.F. is the guarantor of this work, and, as such, had full access to all the data in the study and takes full responsibility for the integrity of the data and the accuracy of data analysis.

Prior Presentation. Parts of this study were presented in abstract form at the 58th German Diabetes Congress, Berlin, Germany, 8–11 May 2024, and at the 84th Scientific Sessions of the American Diabetes Association, Orlando, FL, 21–24 June 2024.

References

1. Sloan G, Selvarajah D, Tesfaye S. Pathogenesis, diagnosis and clinical management of diabetic sensorimotor peripheral neuropathy. Nat Rev Endocrinol 2021;17:400–420

2. Feldman EL, Nave K-A, Jensen TS, Bennett DLH. New horizons in diabetic neuropathy: mechanisms, bioenergetics, and pain. Neuron 2017;93:1296–1313

3. Pafili K, Roden M. Nonalcoholic fatty liver disease (NAFLD) from pathogenesis to treatment concepts in humans. Mol Metab 2021;50:101122

4. Greco C, Nascimbeni F, Carubbi F, Andreone P, Simoni M, Santi D. Association of nonalcoholic fatty liver disease (NAFLD) with peripheral diabetic polyneuropathy: a systematic review and meta-analysis. J Clin Med 2021;10:4466

5. Pham M, Oikonomou D, Hornung B, et al. Magnetic resonance neurography detects diabetic neuropathy early and with proximal predominance. Ann Neurol 2015;78:939–948

6. Pham M, Oikonomou D, Bäumer P, et al. Proximal neuropathic lesions in distal symmetric diabetic polyneuropathy: findings of high-resolution magnetic resonance neurography. Diabetes Care 2011;34:721–723

7. Groener JB, Jende JME, Kurz FT, et al. Understanding diabetic neuropathy—from subclinical nerve lesions to severe nerve fiber deficits: a cross-sectional study in patients with type 2 diabetes and healthy control subjects. Diabetes 2020;69:436–447

8. Jende JME, Groener JB, Oikonomou D, et al. Diabetic neuropathy differs between type 1 and type 2 diabetes: insights from magnetic resonance neurography. Ann Neurol 2018;83:588–598
9. Kender Z, Jende JME, Kurz FT, et al. Sciatic nerve fractional anisotropy and neurofilament light chain protein are related to sensorimotor deficit of the upper and lower limbs in patients with type 2 diabetes. Front Endocrinol (Lausanne) 2023;14:1046690
10. Vaeggemose M, Pham M, Ringgaard S, et al. Magnetic resonance neurography visualizes abnormalities in sciatic and tibial nerves in patients with type 1 diabetes and neuropathy. Diabetes 2017;66:1779–1788
11. Maalmi H, Strom A, Petrera A, et al.; the GDS Group. Serum neurofilament light chain: a novel biomarker for early diabetic sensorimotor polyneuropathy. Diabetologia 2023;66:579–589
12. Schwarz D, Hidmark AS, Sturm V, et al. Characterization of experimental diabetic neuropathy using multicontrast magnetic resonance neurography at ultra high field strength. Sci Rep 2020;10:7593
13. Lundberg E, Borner GHH. Spatial proteomics: a powerful discovery tool for cell biology. Nat Rev Mol Cell Biol 2019;20:285–302
14. Mund A, Brunner A-D, Mann M. Unbiased spatial proteomics with single-cell resolution in tissues. Mol Cell 2022;82:2335–2349
15. Longuespée R, Baiwir D, Mazzucchelli G, Smargiasso N, De Pauw E. Laser microdissection-based microproteomics of formalin-fixed and paraffin-embedded (FFPE) tissues. Methods Mol Biol 2018;1723:19–31
16. Mooshage CM, Schimpfle L, Kender Z, et al. Diametrical effects of glucose levels on microvascular permeability of peripheral nerves in patients with type 2 diabetes with and without diabetic neuropathy. Diabetes 2023;72:290–298
17. Bilotta MT, Petillo S, Santoni A, Cippitelli M. Liver X receptors: regulators of cholesterol metabolism, inflammation, autoimmunity, and cancer. Front Immunol 2020;11:584303
18. Saher G, Brügger B, Lappe-Siefke C, et al. High cholesterol level is essential for myelin membrane growth. Nat Neurosci 2005;8:468–475
19. Gavini CK, Elshareif N, Aubert G, Germanwala AV, Calcutt NA, Mansuy-Aubert V. LXR agonist improves peripheral neuropathy and modifies PNS immune cells in aged mice. J Neuroinflammation 2022;19:57
20. Cermenati G, Giatti S, Cavaletti G, et al. Activation of the liver X receptor increases neuroactive steroid levels and protects from diabetes-induced peripheral neuropathy. J Neurosci 2010;30:11896–11901
21. Elshareif N, Gavini CK, Mansuy-Aubert V. LXR agonist modifies neuronal lipid homeostasis and decreases PGD2 in the dorsal root ganglia in western diet-fed mice. Sci Rep 2022;12:10754
22. Wang S, Dai Y. Roles of AMPK and its downstream signals in pain regulation. Life 2021;11:836
23. Beltramo E, Mazzeo A, Porta M. Thiamine and diabetes: back to the future.? Acta Diabetol 2021;58:1433–1439
24. Hooper PL, Hooper PL. Inflammation, heat shock proteins, and type 2 diabetes. Cell Stress Chaperones 2009;14:113–115
25. Dukay B, Csoboz B, Tóth ME. Heat-shock proteins in neuroinflammation. Front Pharmacol 2019;10:920
26. Slater A, Khattak S, Thomas MR. GPVI inhibition: advancing antithrombotic therapy in cardiovascular disease. Eur Heart J Cardiovasc Pharmacother 2024;10:465–473
27. Gruys E, Toussaint MJM, Niewold TA, Koopmans SJ. Acute phase reaction and acute phase proteins. J Zhejiang Univ Sci B 2005;6:1045–1056
28. Guo S, Moore RM, Charlesworth MC, et al. The proteome of distal nerves: implication in delayed repair and poor functional recovery. Neural Regen Res 2022;17:1998–2006
29. Yi S, Zhang H, Gong L, et al. Deep sequencing and bioinformatic analysis of lesioned sciatic nerves after crush injury. PLoS One 2015;10:e0143491
30. Jiménez CR, Stam FJ, Li KW, et al. Proteomics of the injured rat sciatic nerve reveals protein expression dynamics during regeneration. Mol Cell Proteomics 2005;4:120–132
31. Richner M, Ferreira N, Dudele A, Jensen TS, Vaegter CB, Gonçalves NP. Functional and structural changes of the blood-nerve-barrier in diabetic neuropathy. Front Neurosci 2019;12:1038
32. Chen J-x, Meyrick B. Hypoxia increases Hsp90 binding to eNOS via PI3K-Akt in porcine coronary artery endothelium. Laboratory Investigation 2004;84:182–190
33. Fang F, Wang J, Wang Y-F, Peng Y-D. Microangiopathy in diabetic polyneuropathy revisited. Eur Rev Med Pharmacol Sci 2018;22:6456–6462
34. de Jonge RR, van Schaik IN, Vreijling JP, Troost D, Baas F. Expression of complement components in the peripheral nervous system. Hum Mol Genet 2004;13:295–302
35. Ramaglia V, King RHM, Nourallah M, et al. The membrane attack complex of the complement system is essential for rapid Wallerian degeneration. J Neurosci 2007;27:7663–7672
36. Harhausen D, Khojasteh U, Stahel PF, et al. Membrane attack complex inhibitor CD59a protects against focal cerebral ischemia in mice. J Neuroinflammation 2010;7:15
37. Qiao F, Atkinson C, Kindy MS, et al. The alternative and terminal pathways of complement mediate post-traumatic spinal cord inflammation and injury. Am J Pathol 2010;177:3061–3070
38. Davies CS, Harris CL, Morgan BP. Glycation of CD59 impairs complement regulation on erythrocytes from diabetic subjects. Immunology 2005;114:280–286
39. Warwick CA, Keyes AL, Woodruff TM, Usachev YM. The complement cascade in the regulation of neuroinflammation, nociceptive sensitization, and pain. J Biol Chem 2021;297:101085
40. Tesfaye S, Harris N, Jakubowski JJ, et al. Impaired blood flow and arterio-venous shunting in human diabetic neuropathy: a novel technique of nerve photography and fluorescein angiography. Diabetologia 1993;36:1266–1274